Energy-Efficient Measures to Avoid Downdraft from Large Glazed Facades

Heiselberg, Per; Overby, H.; Bjørn, Erik

Publication date:
1996

Document Version
Publisher's PDF, also known as Version of record

INSTITUTTET FOR BYGNINGSTEKNIK
DEPT. OF BUILDING TECHNOLOGY AND STRUCTURAL ENGINEERING
AALBORG UNIVERSITET • AAU • AALBORG • DANMARK

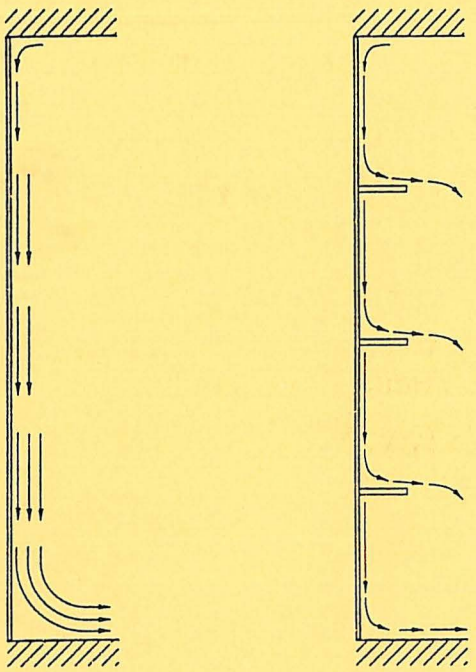

INDOOR ENVIRONMENTAL TECHNOLOGY
PAPER NO. 62

Reprint of ASHRAE Transactions, Vol. 101, Part 2, June 1995

P. HEISELBERG, H. OVERBY & E. BJØRN
ENERGY-EFFICIENT MEASURES TO AVOID DOWNDRAFT FROM LARGE GLAZED FACADES
DECEMBER 1996 ISSN 1395-7953 R9654

The papers on INDOOR ENVIRONMENTAL TECHNOLOGY are issued for early dissemination of research results from the Indoor Environmental Technology Group at the University of Aalborg. These papers are generally submitted to scientific meetings, conferences or journals and should therefore not be widely distributed. Whenever possible reference should be given to the final publications (proceedings, journals, etc.) and not to the paper in this series.

Printed at Aalborg University

INSTITUTTET FOR BYGNINGSTEKNIK
DEPT. OF BUILDING TECHNOLOGY AND STRUCTURAL ENGINEERING
AALBORG UNIVERSITET • AAU • AALBORG • DANMARK

INDOOR ENVIRONMENTAL TECHNOLOGY
PAPER NO. 62

Reprint of ASHRAE Transactions, Vol. 101, Part 2, June 1995

P. HEISELBERG, H. OVERBY & E. BJØRN
ENERGY-EFFICIENT MEASURES TO AVOID DOWNDRAFT FROM LARGE GLAZED FACADES
DECEMBER 1996 ISSN 1395-7953 R9654

ENERGY-EFFICIENT MEASURES TO AVOID DOWNDRAFT FROM LARGE GLAZED FACADES

Per Heiselberg, Ph.D. *Member ASHRAE* **H. Overby, Ph.D.** **Erik Bjorn**

ABSTRACT

Glazed facades may cause thermal discomfort due to downdraft. Convectors placed close to the facade can prevent downdraft but can cause an increase in the energy consumption. The objective of this research was to investigate whether the structural system of a glazed facade can be used to reduce downdraft and avoid thermal comfort problems in the occupied zone.

The effect of large obstacles on a cold boundary layer flow was investigated for different temperature differences between a cold surface and the room air, different distances between the obstacles, and different sizes of the obstacles. The effect of the obstacles was dependent on the characteristics of the flow and the sizes of the obstacles. With turbulent flow and an obstacle larger than the boundary layer thickness, the flow separated from the surface and a new boundary layer was established below the obstacle. The risk of thermal discomfort due to downdraft was reduced considerably.

INTRODUCTION

Glazed facades and atria have become popular as architectural features in building design. They are found in many types of buildings, such as office buildings, hotels, hospitals, and shopping malls. In cold regions they give people the opportunity to perform their daily activities in a naturally lit environment away from the negative effects of a long and cold winter. The use of an atrium can create a thermally compact building where heat loss from the parent building is reduced and passive solar energy gained in the atrium is utilized. Furthermore, both glazed facades and atria can improve the usability of the daylight by allowing it to penetrate deep into the building in the adjacent rooms and thereby reduce the need for electrical lighting. In winter, however, glazed surfaces in buildings in cold regions are often the cause of thermal discomfort, partly due to cold radiation effects and partly due to downdraft problems caused by cold natural convective flows along the surface. For glazed surfaces, the most critical problem is downdraft.

A reduction of the cold natural convective flow can be obtained by increasing the surface temperature of the glass or by neutralizing the flow by a warm air flow in the opposite direction. The surface temperature can be increased passively by reducing the heat loss through the window (more layers of glass, gas filling, low-emission glass). The surface temperature can be increased actively by heating the surface with warm air from convectors close to the surface, by radiant heating, or by electrical heating of the glass. The cold convective airflow can be neutralized with a warm air curtain rising from convectors or supplied through ventilation slits. Common to all the active measures to avoid downdraft is the fact that they increase energy consumption because of the increase in the interior surface temperature and because the active systems also may be operating in periods when general room heating is not needed.

At low windows, downdraft problems can be avoided passively by reducing the heat loss through the window. Heiselberg (1994) has investigated the draft risk in the occupied zone and has developed a draft chart as shown in Figure 1 for low window surfaces.

The interior surface temperature has been calculated for different window types at outdoor temperatures of $\theta_o = 0$°C (32°F) and $\theta_o = -12$°C (10.4°F). In an average year in Denmark the outdoor temperature will be below −12°C (10.4°F) 0.3% of the time and below 0°C (32°F) 15% of the time. Three window types were selected—a double-glazed window, a double-glazed window with one layer of low-emission glass and argon filling, and a triple-glazed window with two layers of low-emission glass and argon filling. The windows have a heat transfer coefficient of $U = 3.0$ W/m^2.°C, $U = 1.6$ W/m^2.°C, and $U = 1.0$ W/m^2.°C (0.53, 0.28, and 0.18 Btu/h.ft^2.°F), respectively. The expected percentage of dissatisfied (PD), due to draft in the occupied zone, can be found as a function of the window type, the outdoor temperature, and the height of the window. For an acceptable PD of 15%, it is seen that a double-glazed window will cause downdraft problems during at least 15% of the year, and for window heights of more than 1 m (3.3 ft), the percentage will be even higher. On the other hand, a double-glazed window with low-emission glass and argon filling will not cause

Per Heiselberg is an associate professor and **Erik Bjorn** is a doctoral student in the Department of Building Technology and Structural Engineering at Aalborg University, Aalborg, Denmark. **H. Overby** is a consulting engineer at Ramboell, Hannemann & Hoejlund A/S, Noerresundby, Denmark.

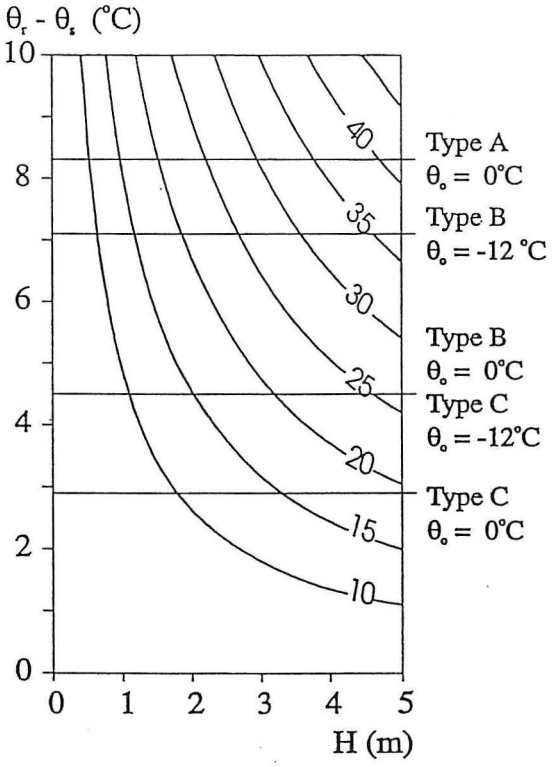

Type A Double glazed window.
Type B Double glazed window with one layer of low emission glass and argon filling.
Type C Triple glazed window with two layers of low emission glass and argon filling.

Figure 1 *The maximum percentage dissatisfied, PD, in the occupied zone of a room with a cold vertical surface and a reference temperature of 22°C as a function of the temperature difference between the reference temperature in the room and the temperature on the surface, Δθ, and of the height of the surface.*

any downdraft problems for a normal window height of 1.25 m (4.1 ft). For window heights equal to normal room height the use of a triple-glazed window with low-emission glass and argon filling will prevent discomfort due to downdraft in the occupied zone. So, for window heights below normal room height it is possible to prevent downdraft problems if the right window type is selected. However, for window heights above normal room height, downdraft problems cannot be prevented by selecting window types with a low heat transfer coefficient; therefore, some kind of active measure will be necessary. The objective of this research was to investigate if the structural system of a glazed facade or an atrium can be used to reduce downdraft and to avoid thermal comfort problems in the occupied zone. Thereby, the initial costs of a convector or ventilation system could be saved and energy consumption could be reduced in the future.

DESCRIPTION OF PRINCIPLE

In ventilated rooms the air inlet device is often placed close to the ceiling. The inlet air forms a wall jet. This jet may be disturbed by ceiling-mounted obstacles such as light fittings or ceiling beams, which, in some cases, cause the air jet to be deflected into the occupied zone. Several authors (Söllner and Klinkenberg 1972; Holmes and Sachariewicz 1973; Nielsen 1980) have presented experimental results that describe the influence of ceiling-mounted obstacles and they have found the critical height of the obstacle at which deflection takes place. The velocity level in the jet will be reduced after the jet has passed the obstacle, and if the height of the obstacle is lower than the critical height the jet will reattach to the ceiling. These observations have led to the question of whether the same phenomena may occur at the boundary layer flow at a vertical wall with obstacles.

The structural system of large glazed facades often includes steel beams close to the surface. Figure 2 shows pictures of two typical glazed facades in Danish buildings. If the gap between the beams in the structural system of the facade and the window frame is covered up, the beams will act as large obstacles for the boundary layer flow. Depending on the width of the obstacle, different flow conditions can be expected to occur. This principle is shown in Figure 3. When the width of the obstacle is smaller than a critical width, the boundary layer flow reattaches to the surface after it has passed the obstacle. The velocity will, however, be reduced; therefore, smaller velocities and an improvement in the thermal comfort can be expected in the occupied zone compared with the situation with a plane surface. When the width of the obstacle is larger than a critical width, the boundary layer flow will separate from the surface after it has passed the obstacle and a new boundary layer flow will be established below the obstacle. The separated airflow will flow into the room probably acting like a cold air jet. In this way, a highly glazed facade can be expected to act as a combination of small individual parts on top of each other. The top parts supply cold air to the room above the occupied zone and the risk of downdraft in the occupied zone is only determined by the flow conditions at the lowest part of the facade.

LABORATORY SETUP

The experiments were conducted in a well-insulated room without mechanical ventilation with the dimensions L by W by H = 4.6 m by 3.0 m by 3.3 m (15.1 ft by 9.8 ft by 10.8 ft). The room was divided into a cold and a warm section by an insulated wall with a window (W × H = 1.2 m × 3.3 m) (3.9 ft × 10.8 ft) placed in the middle (see Figure 4). On the cold side of the window, it was possible to cool down the room to approximately −10°C (14°F) and on the warm side, heating could be supplied and a normal room temperature maintained. The warm section of the room was 3.7 m

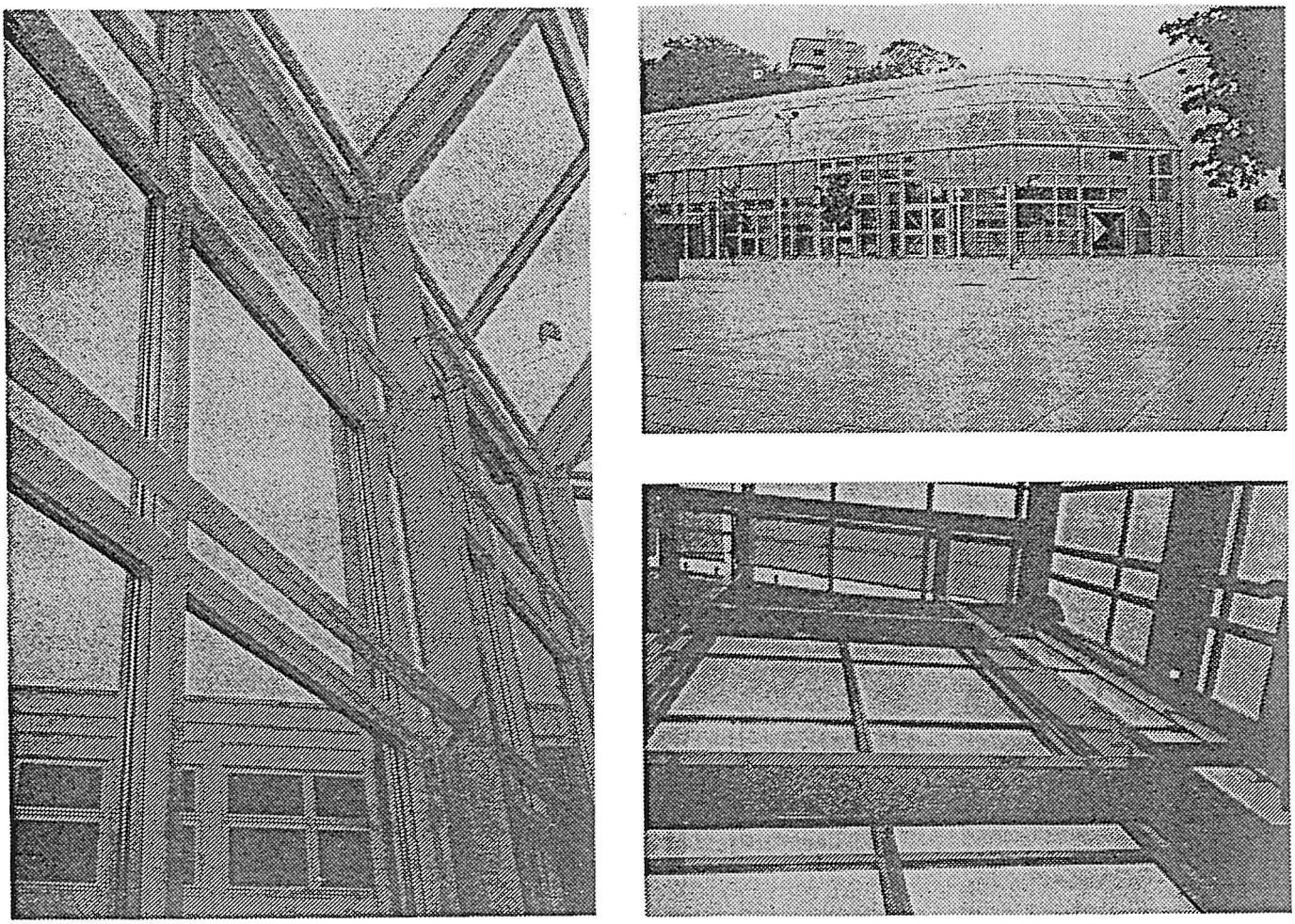

Figure 2 *Two examples of the structural system for glazed facades in Denmark.*

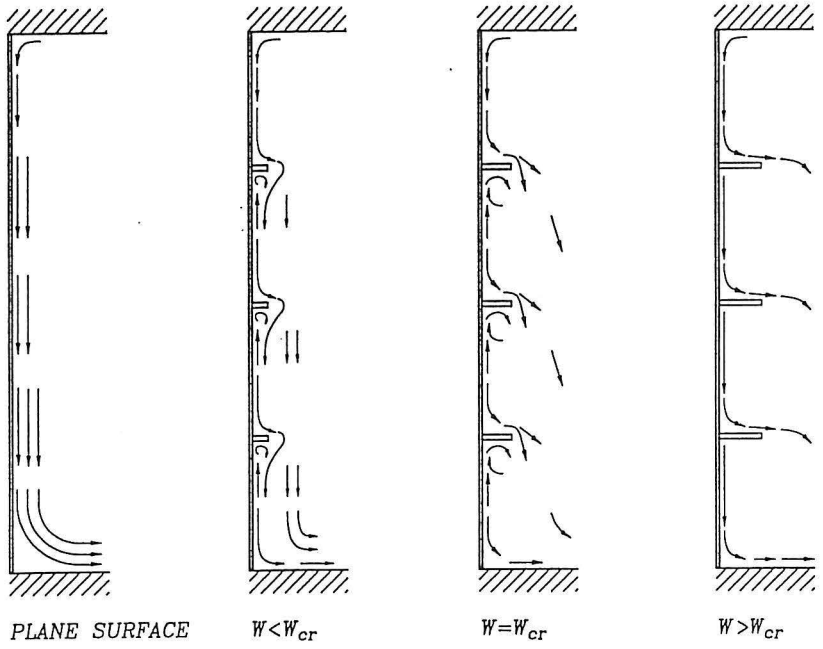

Figure 3 *Principle of flow conditions at a cold vertical wall with different sizes of obstacles.*

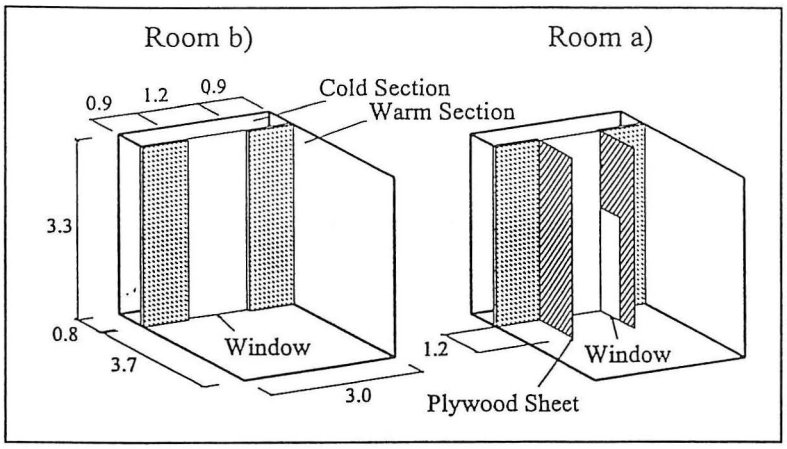

Figure 4 *The test room as used for "realistic" experiments b) and "model" experiments a).*

(12.1 ft) long, and it was in this part that the measurements were carried out. This situation is equivalent to a typical occupied room in a heated building during winter, where the exterior walls and especially the windows are cooler than the room air and the interior surfaces.

The experiments were divided into two categories:

1. Model experiments that were concentrated on the physical impact of rectangular obstacles (in the form of baffle plates) on the boundary layer flow close to the cold window.
2. Experiments that simulated realistic situations where air and surface temperatures, heat loads, etc., were similar to those in a typical office room and where the measurements were concentrated on the effect of the obstacles on the thermal comfort in the occupied zone.

In both types of experiments, temperatures were measured at several heights in the room air, on the window pane, as well as on the other surfaces. The measuring equipment included thermocouples (type K) and a data logger connected to a personal computer. The thermocouples were calibrated to an accuracy of ±0.15°C (0.27°F) in the range of 10°C to 30°C (50°F to 86°F).

In the "realistic" experiments, the mean room temperature was kept nearly constant at 22°C (71.6°F), while the mean surface temperature of the window was varied between 7°C and 13°C (44.6°F and 55.4°F) by changing the temperature in the cold section of the test room. These temperatures are typical of window surface temperatures in Danish buildings during winter. The surface temperature was measured at four heights. The surface temperature distribution was held within ±7% of the average temperature. The average surface temperature did not vary more than 0.2°C (0.36°F) during the measurements. The vertical air temperature difference between 0.2 m and 3.0 m (0.6 ft and 8.6 ft) above the floor was typically between 1°C and 2°C (1.8°F and 3.6°F). The reference room air temperature used in the comparisons was measured 1.6 m (4.6 ft) above the floor. This temperature represented the mean air temperature in the room and did not vary more than 0.2°C (0.36°F) during the measurements.

Temperatures and air velocities were measured in the occupied zone close to the floor, as this is the place where draft problems most likely will arise. Measurements were carried out at distances of 0.4 m to 1.5 m (1.3 ft to 4.9 ft) from the window and at heights of 0.015 m to 0.30 m (0.05 ft to 0.98 ft) with an interval of 5 mm (0.2 in.). The temperatures were measured with thermocouples. The air velocities were measured with hot-sphere anemometers together with a data-processing device calibrated to an accuracy of ±0.025 m/s (4.9 fpm) in the range of 0.05 m/s to 1.0 m/s (9.8 fpm to 197 fpm). The measurements were carried out at a window surface with no obstacles, and at a window surface with obstacles of different sizes and spacing. The width of the obstacles varied between 0.05 m and 0.25 m (0.16 ft and 0.82 ft) and the distances between the obstacles varied between 0.42 m and 0.8 m (1.38 ft and 2.62 ft).

In the model experiments the same room was used but the setup was different. Special care was taken to ensure two-dimensional flow at the window. This was done by placing plywood sheets at each side of the window, perpendicular to the window and extending 1.2 m (3.9 ft) into the room. In each experiment only one obstacle was used, which was placed 1 m (3.3 ft) above the floor. The flow around the obstacle was visualized with white smoke, which was supplied under isothermal conditions and with a very low impulse so it disturbed the flow pattern to a very small extent. The flow pattern was recorded with a video camera.

The room air temperatures and the window surface temperatures were not restricted to "realistic" situations but were chosen together with the height of the window over the obstacle to produce boundary layer flows at different Grashof numbers. To be able to vary the height of the window, an artificial "ceiling" was placed between the plywood sheets. For each Grashof number several obstacles with different widths were tried, the widths varying between 0.05 m and 0.4 m (0.16 ft and 1.31 ft).

MEASUREMENT RESULTS

Model experiments were conducted at 11 combinations of temperature difference ($\Delta\theta$) and window height (h), producing Grashof numbers varying from laminar (Gr_h = $6.9 \cdot 10^8$) to fully turbulent flow ($Gr_h = 1.7 \cdot 10^{10}$). In most situations the flow around an obstacle will follow one of two characteristic patterns. Either the flow will reattach to the window quickly after it has left the edge of the obstacle, creating a recirculating flow immediately under the obstacle, or

the flow will separate completely from the window, following a steep downward curve while mixing with the room air. An intermediate pattern can be observed where the flow is unstable and neither separates properly nor creates the characteristic recirculation zone. This intermediate flow pattern will occur at a certain combination of the Grashof number and the width of the obstacle (see Figure 3). This width was defined as the critical width (w_{cr}) for that particular Grashof number. For each Grashof number, different sizes of obstacles were used to find the critical width. This gave a total of 55 experiments. Figure 5 shows an example of how the increasing width of an obstacle changes the airflow pattern and how the airflow separates from the surface at a certain size of the obstacle. The Grashof number in the experiments is $Gr_h = 5.5 \cdot 10^9$. The width of the plate is 0.1 m (0.33 ft) in picture A. The air reattaches to the surface soon after it has passed the obstacle. In picture B, the width is 0.2 m (0.66 ft). The critical width is obtained and the airflow is beginning to separate. At widths of 0.25 m and 0.3 m (0.82 ft and 0.98 ft) (see pictures C and D), the airflow clearly separates. Critical widths were found for all Grashof numbers except for the most laminar case, where w_{cr} was very large and of no practical interest. Figure 6 shows the critical width as a function of the Grashof number. For the range of Grashof numbers investigated, it is seen that the critical width decreases with increasing Grashof number.

In the situations where separation of the airflow did not occur, a recirculating flow existed. The height (h_R) of the recirculating zone was determined by analysis of the video recording. For this purpose, video recording proved to be superior to photography as the direction of the flow could be determined with much greater accuracy. The height of the recirculating zone h_R seems to be dependent on the Grashof number as well as on the width of the obstacle (see Figure 7). For a given obstacle, h_R will not be smaller than the width of the obstacle. As the Grashof number increases, h_R also increases. This is illustrated by an example in Figure 8 where the width of the obstacle is kept constant at 0.1 m (0.33 ft).

In the "realistic" experiments, velocities and temperatures were measured in the flow above the floor in a series of

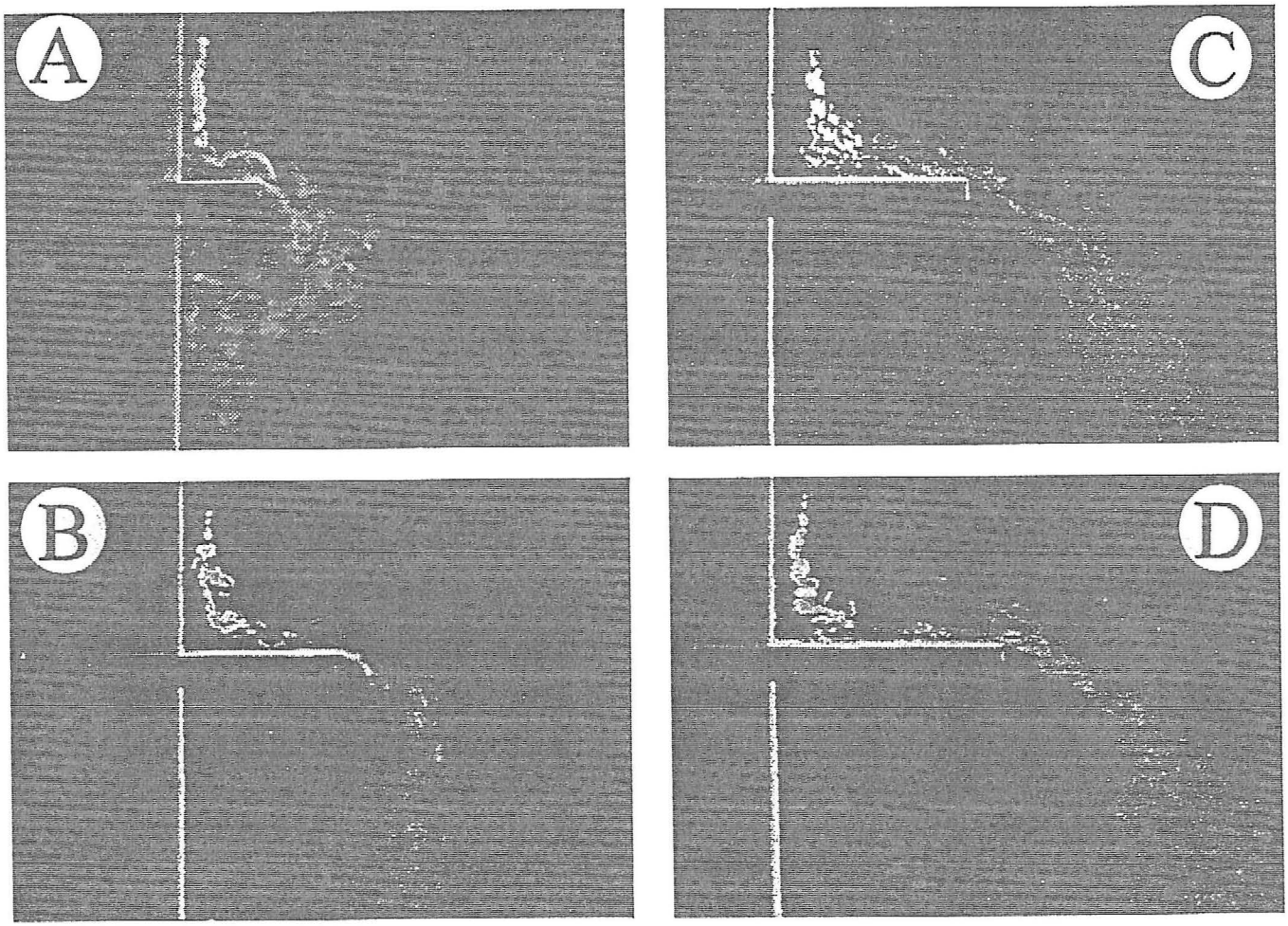

Figure 5 *Flow patterns at obstacles with widths of A) 0.1 m (0.33 ft), B) 0.2 m (0.66 ft), C) 0.25 m (0.82 ft) and D) 0.3 m (0.98 ft). The Grashof number is constant, $Gr_h = 5.5 \cdot 10^9$.*

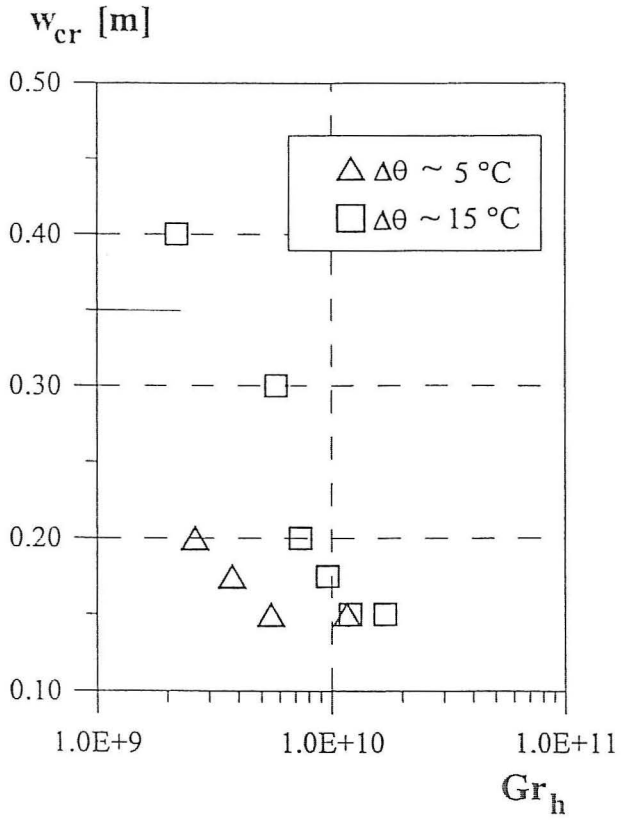

Figure 6 *Critical width of the obstacle as a function of the Grashof number.*

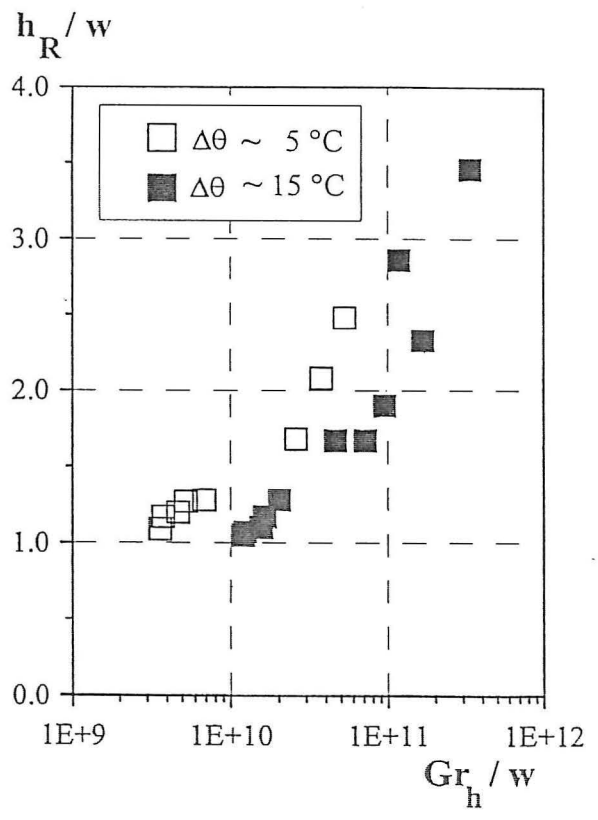

Figure 7 *Height of the recirculation zone as a function of the Grashof number and the width of the obstacle.*

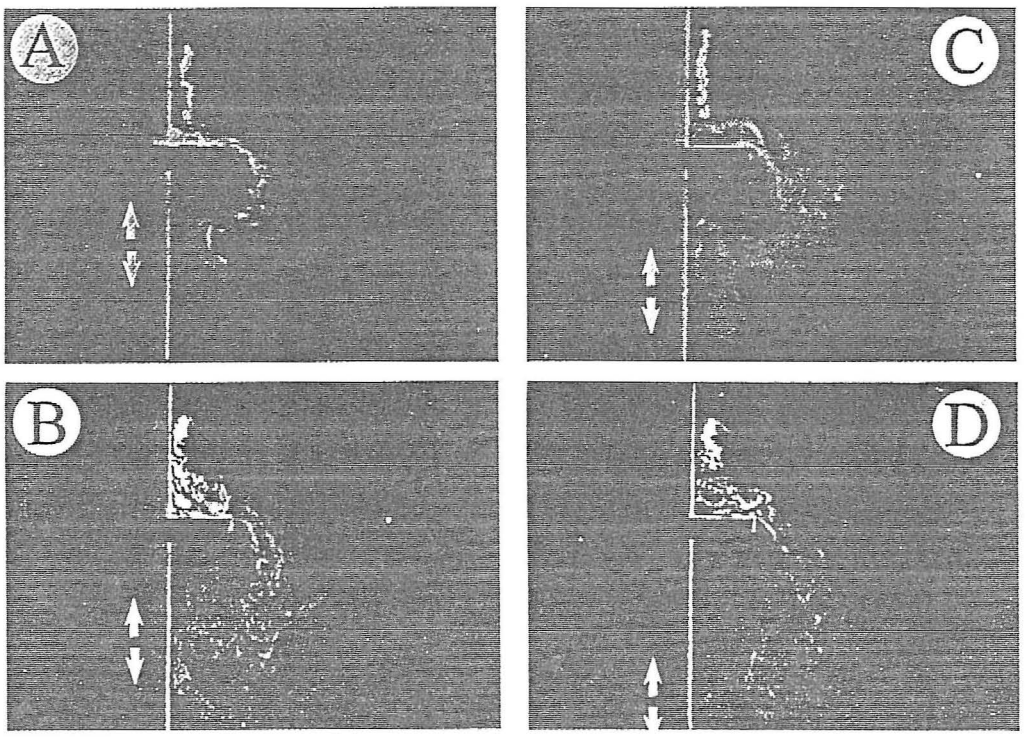

Figure 8 *Flow patterns at an obstacle width of 0.1 m (0.33 ft) and Grashof numbers of A) 6.85· 10^8, B) 2.59· 10^9, C) 5.30· 10^9, and D) 1.16· 10^{10}. The arrows indicate the direction of the flow.*

experiments without the plywood sheets (see Figure 4) and consequently with a three-dimensional airflow. The purpose of this part of the experimental work was to compare the maximum air velocity and the minimum air temperature in the flow at the floor in situations with obstacles on the window to a situation with a plane surface.

Figure 9 shows three different window temperatures, where the maximum velocity measured in the occupied zone (u_{ob}) divided by the maximum velocity calculated for a plane window without obstacles (u_{max}) is shown as a function of the width of the obstacles. In this case the number of obstacles on the window is four, which means that the distance between the obstacles in these experiments is 0.64 m (1.84 ft). The maximum velocities in the occupied zone for the window without obstacles are calculated by Equation 1. This expression is found by Heiselberg (1994) for a three-dimensional case. A standard u_{max} is calculated at the distance 0.6 m (1.72 ft) from the window, which is regarded as the distance from the wall where the occupied zone begins.

$$u_{max}(x) = 0.134\frac{\sqrt{H\,\Delta\theta}}{x+2.04}\ (\text{m/s}) \qquad (1)$$

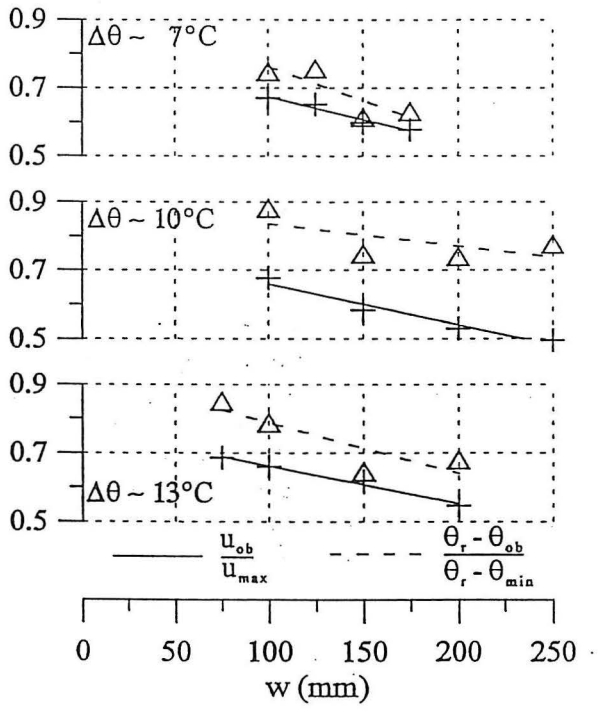

Figure 9 *Reduction of maximum velocity and temperature difference in the occupied zone as a function of the width of the obstacles for temperature differences between the cold surface and room air of Δθ = 7°C, Δθ = 10°C and Δθ = 13°C. The distance between the obstacles at the surface is h = 0.64 m (1.84 ft). Total surface height H = 3.3 m (10.8 ft).*

Figure 9 also shows the temperature difference between the room air (θ_r) and the minimum temperature measured in the occupied zone (θ_{ob}), divided by the temperature difference between the room air (θ_r) and the calculated minimum air temperature in the occupied zone for a window without obstacles (θ_{min}), as a function of the width of the obstacles. The minimum air temperature in the occupied zone for the window without obstacles is calculated by Equation 2. This expression is also used by Heiselberg (1994) for a three-dimensional case. The minimum temperature is also calculated at a distance 0.6 m (1.72 ft) from the window.

$$\theta_{min}(x) = \theta_r - (0.29 - 0.038x)\,(\theta_r - \theta_s)\ (°\text{C}) \qquad (2)$$

Figure 9 shows that small obstacles give less reduction, both in the maximum velocity and in the temperature difference between the room air and the temperature in the flow at the floor. The velocity reduction at different surface temperatures is almost constant for the same width of the obstacles. The reduction of the temperature difference is more unstable in the three cases, but it is significant that large obstacles give a higher minimum temperature in the flow at the floor.

Figure 10 shows the same parameters as in Figure 9. The number of obstacles on the surface is five, which means

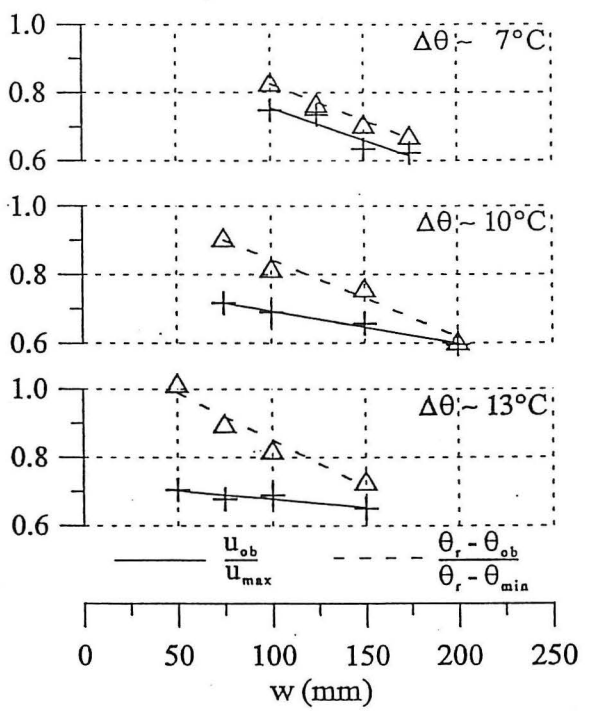

Figure 10 *Reduction of maximum velocity and temperature difference in the occupied zone as a function of the width of the obstacles for temperature differences between the cold surface and room air of Δθ = 7°C, Δθ = 10°C, and Δθ = 13°C. The distance between the obstacles at the surface is h = 0.50 m (1.44 ft). Total surface height H = 3.3 m (10.8 ft).*

that the distance between the obstacles is 0.5 m (1.44 ft). In this situation large obstacles also improve the comfort conditions. By comparing the results in Figure 9 with the results in Figure 10 it can be seen that the velocity and the temperature difference reduction are largest when the number of obstacles is only four (h = 0.64 m) (2.10 ft).

Figure 11 shows the velocity and temperature difference reduction as a function of the number of obstacles for a constant width of the obstacles (0.15 m) (5.9 in.). Here it can be seen that a large number of obstacles at the same surface give less reduction in both the maximum velocity and the minimum temperature in the flow at the floor in the occupied zone.

DISCUSSION

The critical width proved to be greatly dependent on the Grashof number. In the case of laminar flow, Gr_h < approx. 2.10^9 (Cheesewright and Ierokiopitis 1982), the flow was very reluctant to separate and relatively large critical widths were found. With increasing Gr_h, w_{cr} decreased until fully developed turbulence was reached at $Gr_h > 1 - 1.6.10^{10}$ (Cheesewright and Ierokiopitis 1982), where the critical width is approximately equal to the thickness, δ, of the boundary layer calculated (Eckert and Jackson 1951) as

$$\delta = 0.565h\,(Gr)^{-1/10}\,(Pr)^{-8/15}\,[1 + 0.494\,(Pr)^{2/3}]^{1/10}. \quad (3)$$

When comparing with test results from experiments with ceiling-mounted obstacles that deflect turbulent jets, it seems very likely that for turbulent flow the critical width will follow the boundary layer thickness and that it will increase beyond the values shown in Figure 6 if the Grashof number is increased beyond $1.7.10^{10}$, but unfortunately it was not possible to test this with the described test room. Figures 6 and 7 indicate that there was some ambiguity as to the correlation of Gr_h and w_{cr} and of Gr_h and h_R, insofar as experiments with nearly identical Grashof numbers could produce widely differing critical widths and heights of the recirculation zone. This seems to be attributable to the temperature gradients in the test room and on the window. In experiments with a relatively large temperature difference, ($\Delta\theta$ ~ 15°C) (27°F), measurements show a very evenly distributed temperature difference throughout the height of the room. In experiments with a small temperature difference ($\Delta\theta$ ~ 5°C) (9°F), measurements show a more unevenly distributed temperature difference, probably due to stratification effects. This could be the cause of differences in the turbulence of the flow, where a situation with an uneven distribution might create more turbulence. This could explain the results in Figure 6, where the experiments with $\Delta\theta$ ~ 5°C (9°F) apparently reach fully developed turbulence before the experiments with $\Delta\theta$ ~ 15°C (27°F).

The temperatures and the air velocities at the front edge of the obstacle were measured, the temperature with a very thin thermocouple and the air velocity with a slender hot-wire anemometer. If the air that leaves the edge of the obstacle behaved as a two-dimensional jet these parameters would determine the flow pattern. However, in all experiments with separation the airflow followed the same trajectory independent of the air velocity and temperature in the flow. The obstacle was located only 1 m (3.3 ft) above the floor, and at this short distance the airflow path is likely to be affected by the deflection at the floor. Therefore, no conclusion can be drawn on how the trajectory will be in a room after separation.

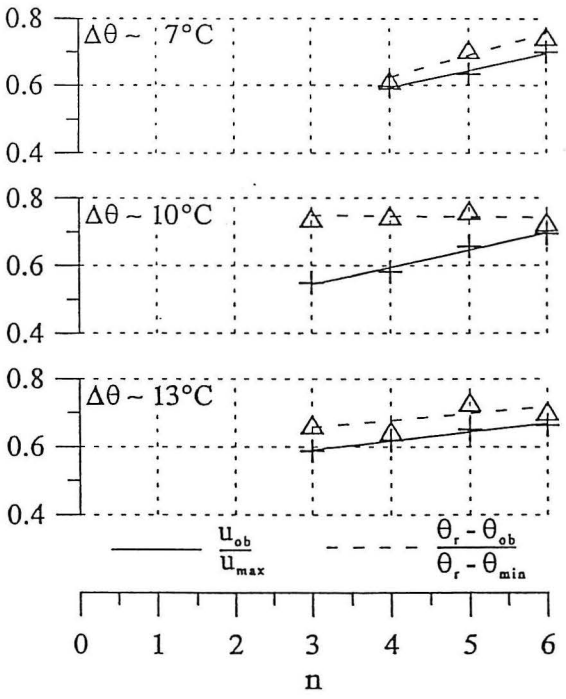

Figure 11 *Reduction of maximum velocity and temperature difference in the occupied zone as a function of the number of obstacles at the surface for temperature differences between the cold surface and room air of $\Delta\theta$ = 7°C, $\Delta\theta$ = 10°C, and $\Delta\theta$ = 13°C. The width of the obstacles was w = 0.15 m (0.49 ft). Total surface height H = 3.3 m (10.8 ft).*

In all experiments with a width of the obstacle less than the critical width, a recirculation zone was established behind the obstacle. The height of the recirculation zone was never less than the width of the obstacle, and it increased with increasing Grashof numbers. The measurements in the occupied zone showed that even if no separation of the boundary layer flow occurred, the presence of the obstacles at the surface reduced the maximum velocity and the temperature difference in the flow and thereby improved the comfort conditions. There seemed to be a correlation between the height of the recirculation zone and the improvement of the comfort conditions, i.e., an increase in the recirculation

height reduced the velocity and the temperature difference in the occupied zone. The measurements showed that reductions between 10% and 40% were obtainable.

Furthermore, the experiments showed that a separation of a laminar boundary-layer flow was not possible in practical applications because the critical width would become too large. In transient and certainly in turbulent boundary-layer flows, the critical width will be reasonable, varying between 0.15 m and 0.30 m (0.49 ft and 0.98 ft). To improve the probability of turbulent flow conditions it is important to have a large distance between the obstacles. The distance should not be less than 2 m (6.6 ft).

The results have been promising, but to develop a design procedure some work is still needed. Almost all experiments were performed at transient flow conditions of the boundary-layer flow. More experiments are needed at turbulent flow conditions to investigate whether the critical width will have the same size as the boundary-layer thickness. It is also necessary to determine how the boundary-layer flow will develop after it has separated from the surface. What will the trajectory look like? How will the velocity level develop? What will be the comfort conditions when the flow reaches the occupied zone? Experiments at a high surface are needed to examine if the idea of a high facade acting as small parts on top of each other is correct.

CONCLUSION

The experiments have shown that use of the structural system as obstacles in the boundary-layer flow is a possible way to improve comfort conditions in the occupied zone in cases with downdraft at glazed facades. If the width of the obstacles is less than the critical width, a recirculation zone will be established behind the obstacle and there will be a reduction of both the maximum velocity and the temperature difference and an improvement of the comfort conditions in the occupied zone. If the width of the obstacle is larger than the critical width, the boundary-layer flow will separate from the surface and a new boundary-layer flow will build up behind the obstacle. The comfort conditions in the occupied zone will in this case not be dependent on the total height of the surface but only on the distance from the lowest obstacle with separation to the floor.

The effect of the obstacles is dependent on the characteristic of the flow and on the size of the obstacle. A separation of the boundary-layer flow from the surface in practical applications requires turbulent flow conditions. To improve the probability of turbulent flow conditions, a distance of more than 2 m (6.6 ft) between the obstacles is needed.

ACKNOWLEDGMENTS

The authors would like to express their appreciation for the contributions from Ivan Anisimov, Klaus Emil Christensen, Jan Jeppesen, and Jakob Wæhrens for their help with the measurements. This research work has been supported financially by the Danish Energy Agency (Energiministeriets forskningsprogram, EFP-93) as part of the cooperative work in IEA-ECB Annex 26, Energy-Efficient Ventilation of Large Enclosures.

NOMENCLATURE

g	=	ravitational acceleration, $g = 9.82$ (m/s^2)
Gr_h	=	local Grashof number ($Gr_h = g\ \beta\ \Delta\ \theta\ h^3/\nu^2$)
h	=	spacing between obstacles (m)
h_R	=	recirculation length (height) of flow behind obstacle (m)
H	=	surface height (m)
u_{max}	=	calculated maximum velocity in the occupied zone for plane surface (m/s)
u_{ob}	=	measured maximum velocity in the occupied zone for surface with obstacles (m/s)
w	=	width of obstacle (m)
w_{cr}	=	critical width of obstacle (m)
β	=	volumetric expansion coefficient (K^{-1})
δ	=	boundary layer thickness (m)
ν	=	kinematic viscosity (m^2/s)
θ_{min}	=	calculated minimum temperature in the occupied zone for plane surface (°C)
θ_{ob}	=	measured minimum temperature in the occupied zone for surface with obstacles (°C)
θ_r	=	room air temperature (°C)
θ_s	=	surface temperature (°C)
$\Delta\theta$	=	temperature difference between room air and surface (°C)

REFERENCES

Cheesewright, R., and E. Ierokiopitis. 1982. Velocity measurements in a turbulent natural convection boundary layer. *Int. Heat Transfer Conf. Munchen*, vol. 2, pp. 305-309.

Eckert, E.R.G., and T.W. Jackson. 1951. Analysis of turbulent free-convection boundary layer on flat plate. NACA-Report 1015.

Heiselberg, P. 1994. Draught risk from cold vertical surfaces. *Building and Environment* 29(3): 297-301.

Holmes, M.J., and E. Sachariewicz. 1973. The effect of ceiling beams and light fittings on ventilating jets. Laboratory Report No. 79. HVRA.

Nielsen, P.V. 1980. The influence of ceiling-mounted obstacles on the air flow pattern in air-conditioned rooms at different heat loads. *Building Services Engineering Research & Technology* 1(4).

Söllner, G., and K. Klinkenberg. 1972. Leuchten als Storkorper im Luftstrom (Lighting fixtures as obstacles in air flow). *Heizung, Luftung/Klimatechnik Haustechnik* 23(4).

PAPERS ON INDOOR ENVIRONMENTAL TECHNOLOGY

PAPER NO. 34: T. V. Jacobsen, P. V. Nielsen: *Numerical Modelling of Thermal Environment in a Displacement-Ventilated Room.* ISSN 0902-7513 R9337.

PAPER NO. 35: P. Heiselberg: *Draught Risk from Cold Vertical Surfaces.* ISSN 0902-7513 R9338.

PAPER NO. 36: P. V. Nielsen: *Model Experiments for the Determination of Airflow in Large Spaces.* ISSN 0902-7513 R9339.

PAPER NO. 37: K. Svidt: *Numerical Prediction of Buoyant Air Flow in Livestock Buildings.* ISSN 0902-7513 R9351.

PAPER NO. 38: K. Svidt: *Investigation of Inlet Boundary Conditions Numerical Prediction of Air Flow in Livestock Buildings.* ISSN 0902-7513 R9407.

PAPER NO. 39: C. E. Hyldgaard: *Humans as a Source of Heat and Air Pollution.* ISSN 0902-7513 R9414.

PAPER NO. 40: H. Brohus, P. V. Nielsen: *Contaminant Distribution around Persons in Rooms Ventilated by Displacement Ventilation.* ISSN 0902-7513 R9415.

PAPER NO. 41: P. V. Nielsen: *Air Distribution in Rooms - Research and Design Methods.* ISSN 0902-7513 R9416.

PAPER NO. 42: H. Overby: *Measurement and Calculation of Vertical Temperature Gradients in Rooms with Convective Flows.* ISSN 0902-7513 R9417.

PAPER NO. 43: H. Brohus, P. V. Nielsen: *Personal Exposure in a Ventilated Room with Concentration Gradients.* ISSN 0902-7513 R9424.

PAPER NO. 44: P. Heiselberg: *Interaction between Flow Elements in Large Enclosures.* ISSN 0902-7513 R9427.

PAPER NO. 45: P. V. Nielsen: *Prospects for Computational Fluid Dynamics in Room Air Contaminant Control.* ISSN 0902-7513 R9446.

PAPER NO. 46: P. Heiselberg, H. Overby, & E. Bjørn: *The Effect of Obstacles on the Boundary Layer Flow at a Vertical Surface.* ISSN 0902-7513 R9454.

PAPER NO. 47: U. Madsen, G. Aubertin, N. O. Breum, J. R. Fontaine & P. V. Nielsen: *Tracer Gas Technique versus a Control Box Method for Estimating Direct Capture Efficiency of Exhaust Systems.* ISSN 0902-7513 R9457.

PAPER NO. 48: Peter V. Nielsen: *Vertical Temperature Distribution in a Room with Displacement Ventilation.* ISSN 0902-7513 R9509.

PAPER NO. 49: Kjeld Svidt & Per Heiselberg: *CFD Calculations of the Air Flow along a Cold Vertical Wall with an Obstacle.* ISSN 0902-7513 R9510.

PAPER NO. 50: Gunnar P. Jensen & Peter V. Nielsen: *Transfer of Emission Test Data from Small Scale to Full Scale.* ISSN 1395-7953 R9537.

PAPER NO. 51: Peter V. Nielsen: *Healthy Buildings and Air Distribution in Rooms.* ISSN 1395-7953 R9538.

PAPERS ON INDOOR ENVIRONMENTAL TECHNOLOGY

PAPER NO. 52: Lars Davidson & Peter V. Nielsen: *Calculation of the Two-Dimensional Airflow in Facial Regions and Nasal Cavity using an Unstructured Finite Volume Solver.* ISSN 1395-7953 R9539.

PAPER NO. 53: Henrik Brohus & Peter V. Nielsen: *Personal Exposure to Contaminant Sources in a Uniform Velocity Field.* ISSN 1395-7953 R9540.

PAPER NO. 54: Erik Bjørn & Peter V. Nielsen: *Merging Thermal Plumes in the Indoor Environment.* ISSN 1395-7953 R9541.

PAPER NO. 55: K. Svidt, P. Heiselberg & O. J. Hendriksen: *Natural Ventilation in Atria - A Case Study.* ISSN 1395-7953 R9647.

PAPER NO. 56: K. Svidt & B. Bjerg: *Computer Prediction of Air Quality in Livestock Buildings.* ISSN 1395-7953 R9648.

PAPER NO. 57: J. R. Nielsen, P. V. Nielsen & K. Svidt: *Obstacles in the Occupied Zone of a Room with Mixing Ventilation.* ISSN 1395-7953 R9649.

PAPER NO. 58: C. Topp & P. Heiselberg: *Obstacles, an Energy-Efficient Method to Reduce Downdraught from Large Glazed Surfaces.* ISSN 1395-7953 R9650.

PAPER NO. 59: L. Davidson & P. V. Nielsen: *Large Eddy Simulations of the Flow in a Three-Dimensional Ventilated Room.* ISSN 1395-7953 R9651.

PAPER NO. 60: H. Brohus & P. V. Nielsen: *CFD Models of Persons Evaluated by Full-Scale Wind Channel Experiments.* ISSN 1395-7953 R9652.

PAPER NO. 61: H. Brohus, H. N. Knudsen, P. V. Nielsen, G. Clausen & P. O. Fanger: *Perceived Air Quality in a Displacement Ventilated Room.* ISSN 1395-7953 R9653.

PAPER NO. 62: P. Heiselberg, H. Overby & E. Bjørn: *Energy-Efficient Measures to Avoid Downdraft from Large Glazed Facades.* ISSN 1395-7953 R9654.

PAPER NO. 63: O. J. Hendriksen, C. E. Madsen, P. Heiselberg & K. Svidt: *Indoor Climate of Large Glazed Spaces.* ISSN 1395-7953 R9655.

PAPER NO. 64: P. Heiselberg: *Analysis and Prediction Techniques.* ISSN 1395-7953 R9656.

PAPER NO. 65: P. Heiselberg & P. V. Nielsen: *Flow Element Models.* ISSN 1395-7953 R9657.

PAPER NO. 66: Erik Bjørn & P. V. Nielsen: *Exposure due to Interacting Air Flows between Two Persons.* ISSN 1395-7953 R9658.

PAPER NO. 67: P. V. Nielsen: *Temperature Distribution in a Displacement Ventilated Room.* ISSN 1395-7953 R9659.

PAPER NO. 68: G. Zhang, J. C. Bennetsen, B. Bjerg & K. Svidt: *Analysis of Air Movement Measured in a Ventilated Enclosure.* ISSN 139995-7953 R9660.

Department of Building Technology and Structural Engineering
Aalborg University, Sohngaardsholmsvej 57. DK 9000 Aalborg
Telephone: +45 9635 8080 Telefax: +45 9814 8243